N65 29847

(PAGES) 32

(NASA CR OR TMX OR AD NUMBER)

(THRU)

(CODE) 29

(CATEGORY)

LATITUDINAL VARIATIONS
OF ELECTRON TEMPERATURE
AND CONCENTRATION
FROM SATELLITE PROBES

BY

L. H. BRACE
B. M. REDDY

MAY 1965

NASA ——— GODDARD SPACE FLIGHT CENTER ———

GREENBELT, MARYLAND

LATITUDINAL VARIATIONS OF ELECTRON TEMPERATURE AND CONCENTRATION FROM SATELLITE PROBES

by

L. H. Brace and B. M. Reddy

May 1965

CONTENTS

LIST OF FIGURES

LATITUDINAL VARIATIONS OF ELECTRON TEMPERATURE
AND CONCENTRATION FROM SATELLITE PROBES

ABSTRACT

29847

Measurements of electron temperature (T_e) and concentration (N_e) have been made by the use of cylindrical electrostatic probes on the Explorer XXII satellite, which was launched in October 1964. Since the satellite is in an 80° inclination, nearly circular orbit at 1000 kilometers altitude, the latitudinal structure of the ionosphere is most easily determined. The measurements reveal a remarkable symmetry about the magnetic equator which suggests a strong degree of geomagnetic control. In the daytime a maximum of N_e occurs at the equator (≈ 3-4×10^4/cc), and N_e decreases to a minimum at 50–60°N and S magnetic latitude ($\approx 1 \times 10^4$/cc). In the daytime, T_e varies somewhat inversely with N_e, reaching a maximum at 50°-60° (≈ 3000°K), a minimum at the equator (≈ 2400°K), and decreasing in the polar regions. At night, the equatorial maximum disappears and pronounced maxima develop at about 35–40° latitude ($\approx 3 \times 10^4$/cc). A steep gradient at higher latitudes ends in a deep trough in the auroral zone ($\approx 10^3$/cc). The nighttime T_e remains very low (≈ 800°K) at low and middle latitudes but rises steeply near the auroral trough (≈ 2500°K) and decreases at higher latitudes. The mean ion mass, inferred from the ion current measurements, suggest that H^+ is the dominant ion at the equator and O^+ predominates above 40° magnetic latitude. Small scale fluctuations of the electron currents to the probes during some of the polar region measurements reveal fine irregularities in N_e along the satellite path. These irregularities occur primarily in the midnight to sunrise period and have horizontal dimensions of only a few hundred meters and amplitudes of up to 30%. Nearly all occur poleward of the auroral zone.

Author

LATITUDINAL VARIATIONS OF ELECTRON

TEMPERATURE AND CONCENTRATION FROM

SATELLITE PROBES

by

L. H. Brace and B. M. Reddy*

INTRODUCTION

On October 9, 1964, Explorer XXII, the ionosphere beacon satellite,[1,2] was launched into an 80° inclination direct orbit which was nearly circular at an altitude of 1000 kilometers. The primary mission of the satellite was to permit radio propagation studies of the ionosphere on a global scale. The beacon experiment, radiating at 20, 40 and 41 megacycles, permits determination of the total electron content in the region between the satellite and an observing station on the ground. Knowledge of the electron density (N_e) at the satellite is very useful in the interpretation of beacon data, and for this reason two cylindrical electrostatic probes were employed to permit direct "in situ" measurements of the local plasma. It is the purpose of this paper to describe the probe experiment and to report some of the early results. No attempt will be made here to discuss the detailed implications of these results, since more intensive study of the data is required before this can be done.

THE EXPERIMENT

Figure 1 shows the mounting position of the probes and the electrical system employed. The satellite is stabilized by a passive magnetic system which causes the spin axis to remain aligned with the local geomagnetic field, somewhat like the needle of a compass. Thus, one end of the satellite always points generally northward and the other end points southward. To insure undisturbed measurements when the satellite is moving either north or south, one sensor was mounted on each end of the satellite, as shown.

*Fellow of the National Academy of Sciences.

Figure 1—Block diagram of cylindrical electrostatic probe experiment on the Explorer XXII satellite. A sawtooth voltage (V_a) is applied to either of two collectors, and the resulting current from the plasma is measured by either of two linear response current detectors whose outputs are telemetered to Earth.

The Experimental Arrangement

The experiment is essentially identical to that employed on the Explorer XVII satellite[3] and several rocket flights.[4] In this application, a 2 cps sawtooth voltage (-3v to +5v) is applied in series with either of two independent linear current detectors which are in turn connected alternately to each of the cylindrical probes. The sensor consists of a 5-inch guard electrode and 9-inch collector of 0.022 inches diameter. The guard prevents the collection of current in the region immediately adjacent to the spacecraft, and therefore avoids any possible related disturbance of the measurements. The collector dimensions are such that the probe operates in an orbital-motion-limited mode in which the simple Langmuir probe equations for a cylinder are applicable.[5]

The net current to the collector is the sum of the ion and electron currents and in the sunlight, a small component of photoemission. When the collector is a few volts negative with respect to the plasma, the thermal electrons are entirely rejected and the probe is said to be <u>ion saturated</u>. The ion current to a stationary cylindrical probe is given by

$$I_i = A N_i \, e \, (kT_i/2\pi m_i)^{1/2} \cdot \frac{2}{\pi^{1/2}} \, (1 + eV/kT_i)^{1/2}, \quad (eV/kT > 2) \tag{1}$$

where

I_i, is the ion current,

A, the probe area,

N_i, the ion concentration,

e, the electron charge,

k, the Boltzman constant,

T_i, the ion temperature,

m_i, the ion mass and

V, the potential of the probe relative to plasma.

In the ion saturation region, $eV/kT_i \gg 1$, therefore (1) reduces to

$$I_i = \frac{A N_i \, e}{\pi} \, (2 \, eV/m_i)^{1/2} \tag{2}$$

It is interesting to note that the slope of the ion saturation region depends upon $N_i/m_i^{1/2}$; i.e.,

$$dI_i/dV = \frac{Ae}{\pi} \, (2e/V)^{1/2} \, N_i/m_i^{1/2}, \quad |eV/kT_e| \gg 1 \tag{3}$$

so that, when the ion (or electron) concentration is known, the ion mass obtains from the slope of the ion current characteristic. It should be pointed out that

the existence of a fixed component of photoemission will not affect the ion current slope.

A possible source of error in applying (2) and (3) to satellite probe data is the high translational velocity of the probe with respect to the plasma. The stationary probe equations are most applicable when the ion thermal velocity is comparable to or greater than the translational velocity and this is true only for He^+ and H^+. Until further study of the effects of velocity upon ion current are carried out, the slope of I_i should be regarded only as an indication of ion mass. Future use of this experiment along with high resolution ion mass spectrometers on the same spacecraft is expected to provide the best evidence for understanding the effects of velocity on the ion current slope.

At the other extreme of the applied voltage sweep, when the probe is driven positive with respect to the plasma such that it attracts electrons, it is said to be <u>electron saturated</u>, and the saturation equation again applies

$$I_e = \frac{A N_e e}{\pi} (2eV/m_e)^{1/2}, \qquad |eV/kT_e| >> 1 \qquad (4)$$

Equation (4) is the primary means by which the electron concentration, N_e, is derived from volt-ampere characteristics. Between the ion and electron saturation regions lies the <u>electron retardation region</u> which is employed for the measurement of electron temperature (T_e). In this region I_e is given by

$$I_e = A N_e e (kT_e/2\pi m_e)^{1/2} \exp(eV/kT_e), \quad V < 0 \qquad (5)$$

and T_e is given by

$$T_e = -\frac{e}{k} \frac{dV}{d(\ln I_e)} \qquad (6)$$

Figure 2 is a photograph of a one-second segment of telemetry record which shows a pair of volt-ampere curves measured at moderate temperature and concentration. The plasma potential (V_p), from which the probe potential is measured, is identified as the inflection point of the curve. At the far left of each curve is the ion saturation region which establishes the reference level from
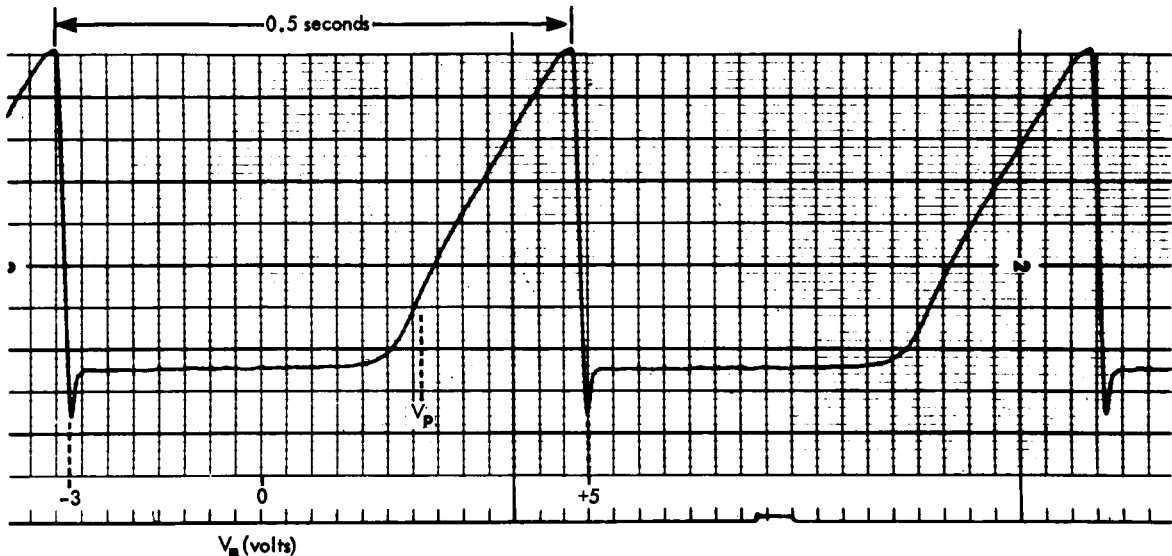
Figure 2—Photo of one second of telemetry record showing a pair of volt-ampere characteristics from which N_e, T_e and m_i are derived. The high current detector (0.3μa full scale) was employed.

which I_e is measured and which permits m_i to be derived. Immediately to the left of V_p is the exponential electron retardation region from which T_e is derived. To the right is the electron saturation region which permits N_e to be measured.

The average electron concentration at 1000 kilometers provides an ion current too small to be resolved with the high current detector, therefore little slope is visible in the ion saturation regions of Figure 2. Figure 3 shows a pair of curves recorded only five seconds later in the same pass and employing the low current detector. This higher sensitivity detector permits the ion slope to be measured and also provides increased resolution of the electron retardation region which is needed for T_e measurements when N_e is low.

The sensitivities employed permit resolution of the electron saturation region in the density range $1 \times 10^2 < N_e < 3 \times 10^4$/cc, which was expected to encompass the variations encountered in a 1000 km circular, polar orbit. However, N_e sometimes exceeds 3×10^4/cc, and much of the electron saturation region exceeds full scale and is lost. In these cases, N_e is derived using (5) and the electron current at the plasma potential, which is only about 20% of the current

Explorer XXII Volt-ampere characteristics
High T_e
Low Current Channel

0.5 sec

-3

0

+5

V_B(volts)
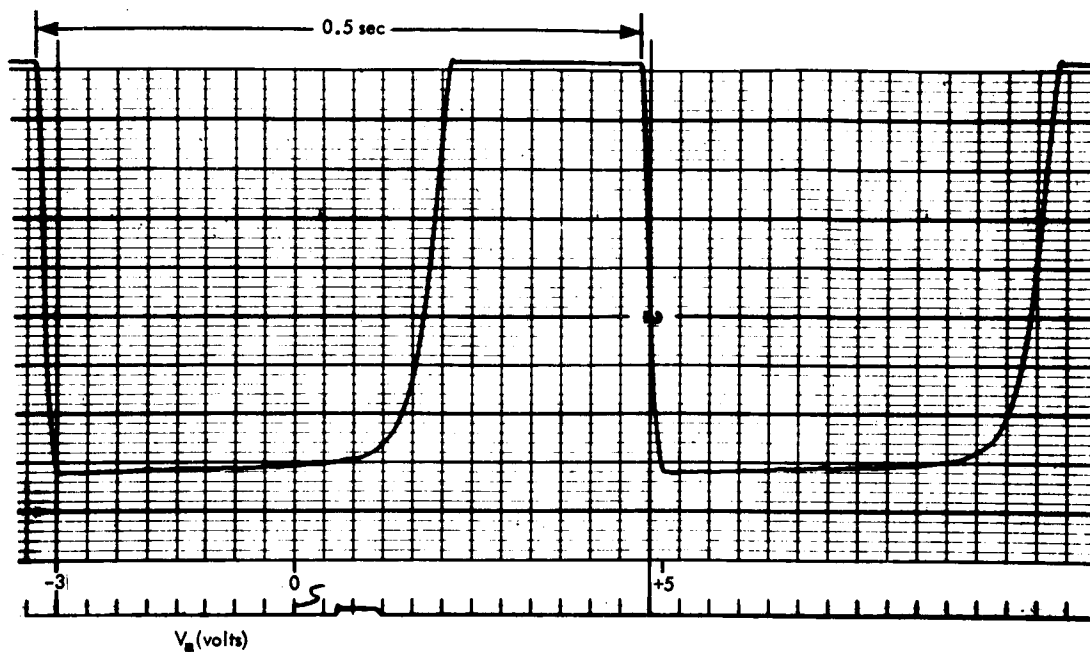
Figure 3–Photo of one second of telemetry record for the same burst of data as shown in
Figure 2, but employing the low current detector (0.05 μa full scale).

at the maximum positive voltage. However, this alternate method is somewhat
less accurate than the electron saturation method because of the steepness of
the electron current characteristic near V_p and a ± 0.1 volt uncertainty in the
identification of V_p. The resulting error in N_e for such cases may be as much
as 20%. The same uncertainty in identifying V_p causes less than 5% error in
the saturation method which is employed when $N_e < 3 \times 10^4$/cc.

The Measurement Sequence

The entire measurement sequence in which each probe is connected alter-
nately to each detector requires 10 seconds and is repeated twice during each
operation of the experiment. To conserve power and telemetry capacity, an
automatic programmer in the spacecraft energizes the experiment every three
minutes continuously throughout the lifetime of the satellite. Thus, each pass
of the satellite consists of several short bursts of probe data, transmitted at
about 1200 kilometer intervals along the orbit. Figure 4 is a photo of a section

EXPLORER XXII
RAW ELECTROSTATIC PROBE DATA

MEASUREMENTS

CALIBRATION 0.3 μa
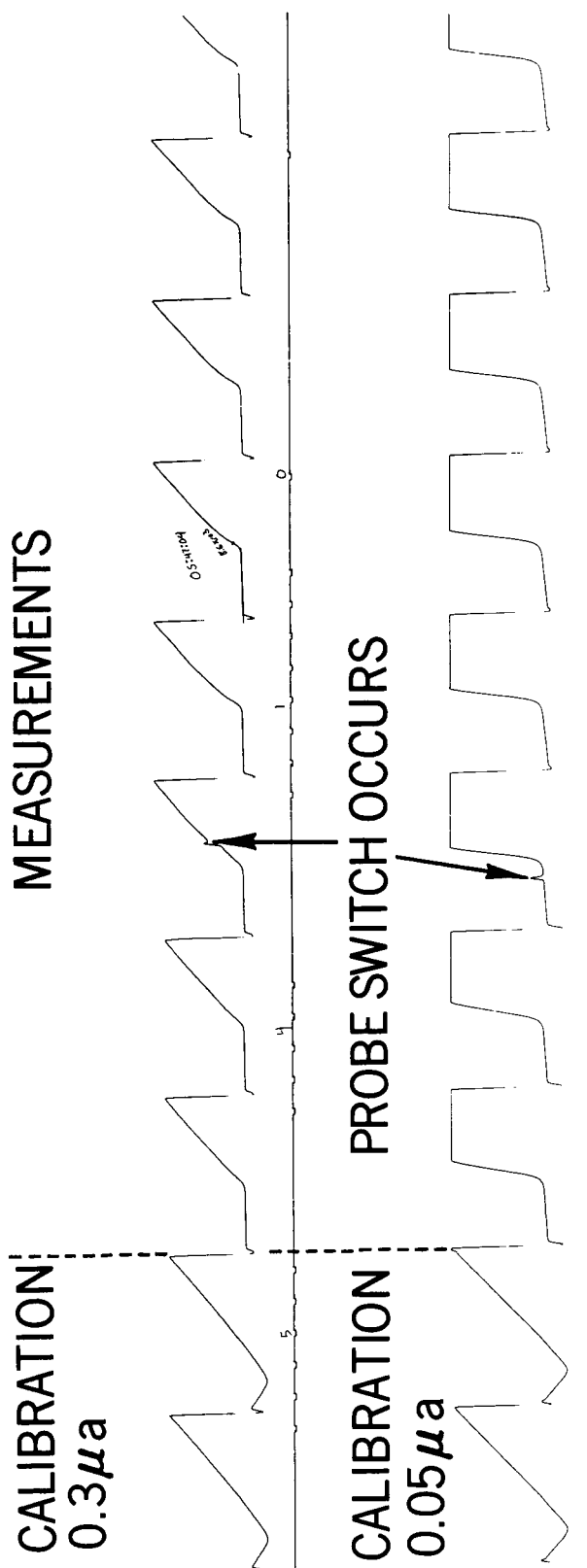
PROBE SWITCH OCCURS

CALIBRATION 0.05 μa

Figure 4-Photo of telemetry record showing 10 seconds of data representing one full sampling cycle in which each probe is connected to each detector, following an inflight calibration. The electron concentration here was approximately 1×10^4/cc.

of telemetry record showing several seconds of raw data from a single burst which helps illustrate the data sampling sequence. Each series of measurements begins with an inflight current calibration which is obtained by the substitution of appropriate resistances in place of the probes. A calibration occurs automatically every five seconds as the alternate detector is placed in the measurement circuit. Following calibration, the detector is connected first to one probe and then to the other, a transition normally accompanied by a small switching transient visible in Figure 4. In this case, the $0.3\mu a$ detector would be employed for N_e and the $0.05\mu a$ detector would provide T_e and m_i measurements.

THE RESULTS

At the time of this writing N_e and T_e have been derived for about 400 passes (approximatly 1600 bursts) of Explorer XXII data which have occurred between October 10 and January 7, 1965. These data represent a wide range of latitude, longitude and local time and are generally descriptive of the ionosphere at an altitude of approximately 1000 kilometers, in northern winter. Data were recorded at the following NASA Stadan stations:

> Blossom Point, Maryland
> Fort Myers, Florida
> Newfoundland
> Grand Forks, North Dakota
> College, Alaska
> Mojave, California
> Quito, Equador
> Lima, Peru
> Santiago, Chile
> Winkfield, England
> Johannesburg, South Africa
> Woomera, Australia

The polar orbit, and its near circularity, makes the latitudinal structure particularly evident in the resulting measurements. For this reason we have plotted the data as a function of geomagnetic latitude. The behavior of the ionosphere with respect to other variables then appears largely as differences in the latitudinal structure. To minimize the effects of local time, we have plotted only the data corresponding to the relatively stable periods following local noon and midnight.

Actual Data Points

Figures 5 and 6 show the N_e and T_e data points from all longitudes for the period 000 - 0330 hours in November and December of 1964. The individual points from a particular pass are joined by lines to approximate the instantaneous latitudinal structure existing during the pass and to identify the points as belonging to particular passes. The long and short dashes represent data from the stations along the 75th meridian (50°W - 100°W), and only at these longitudes was it possible to obtain complete pole to pole coverage. The short dashed lines represent Woomera and some of the College passes (110°E - 150°E), and the solid lines represent Johannesburg and Winkfield passes (50°E - 50°W). .Finally, the long dashes represent data from the western U.S. and Canada recorded at Mojave and College (100°W - 130°W). The ionospheric N_e structure in this range of longitudes was sufficiently different from that of the 75th meridian to warrant plotting it separately. It should be stressed that this particular means of sorting the data by longitude arises not so much from the characteristics of the ionosphere but more from the geographic distribution of the various STADAN stations which recorded the data. Indeed most of the spread in N_e within each of the stated ranges remains longitudinal in origin. In at least one pass (labelled D), deviations have been correlated with high values of the 3-hour magnetic index a_p. In this case, the disturbance was associated with an enhancement of N_e in the equatorial region.

Gross Latitudinal Structure

Plots similar to Figures 5 and 6 have also been prepared for the daytime data (1200-1530 hours) in November and December of 1964. Figures 7, 8, 9 and 10 summarize the gross latitudinal structure of the ionosphere both day and night at the selected longitudes. These graphs generally outline the extremes of N_e and T_e found in the given longitude ranges and are intended primarily to convey the predominant features of the ionosphere at 1000 ±100 km during this period.

The Mean Ion Mass

Figure 11 shows the ion mass m_i derived from the slope of the ion saturation curves, with the associated standard deviations of the values. Since the nighttime N_e is too low to permit the slope to be determined at all latitudes, Figure 11 represents only daytime data. Similar, but preliminary, results have been obtained at midlatitudes at night however.
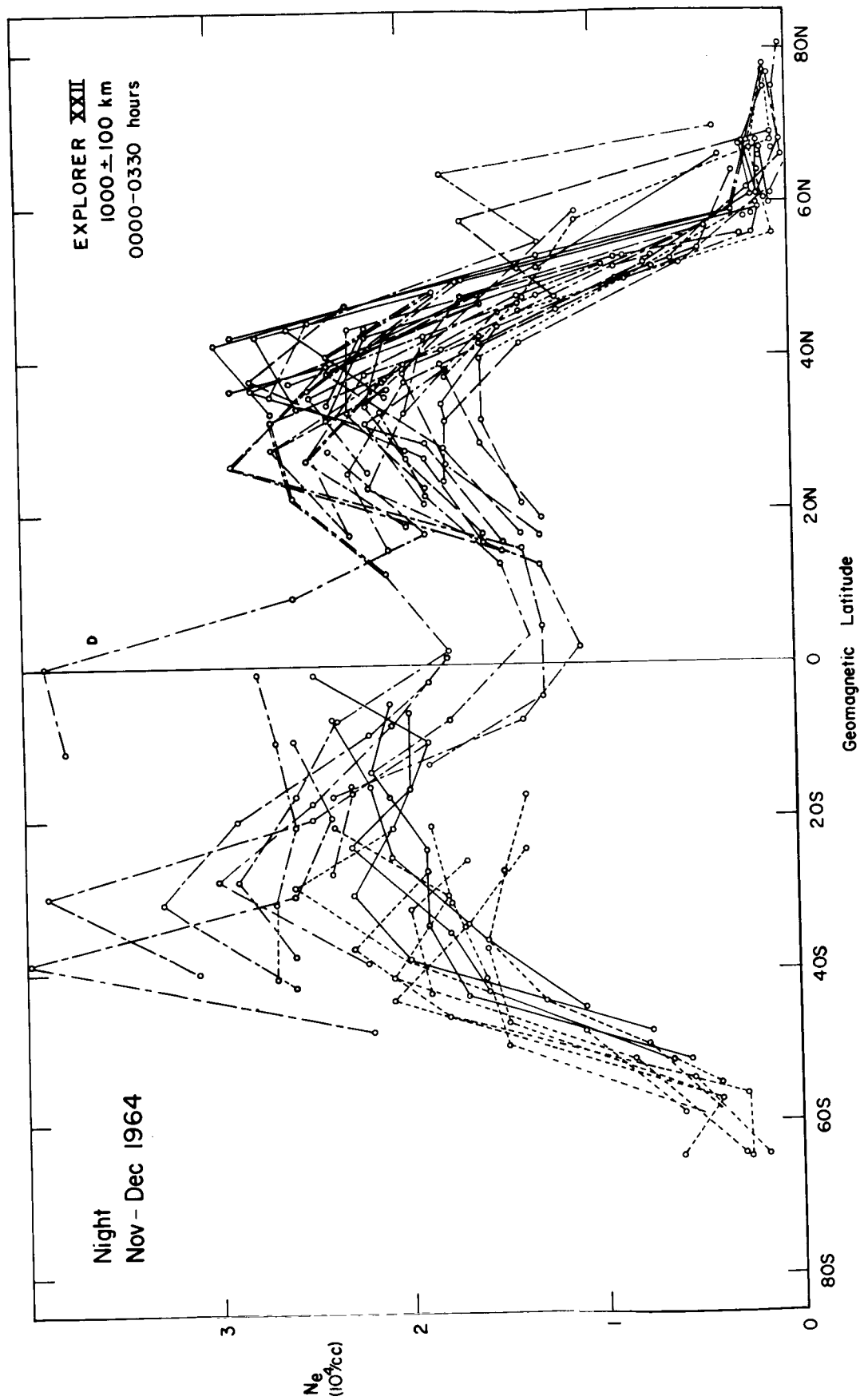
Figure 5—Raw values of N_e in the post midnight period at all available longitudes. The individual points from single passes are joined by lines to approximate the instantaneous latitudinal profile they represent. The various passes, coded by longitude as discussed in the text, show strong longitudinal dependence superposed on the larger latitudinal variations in N_e. The pass labelled D corresponds to a magnetically disturbed day.
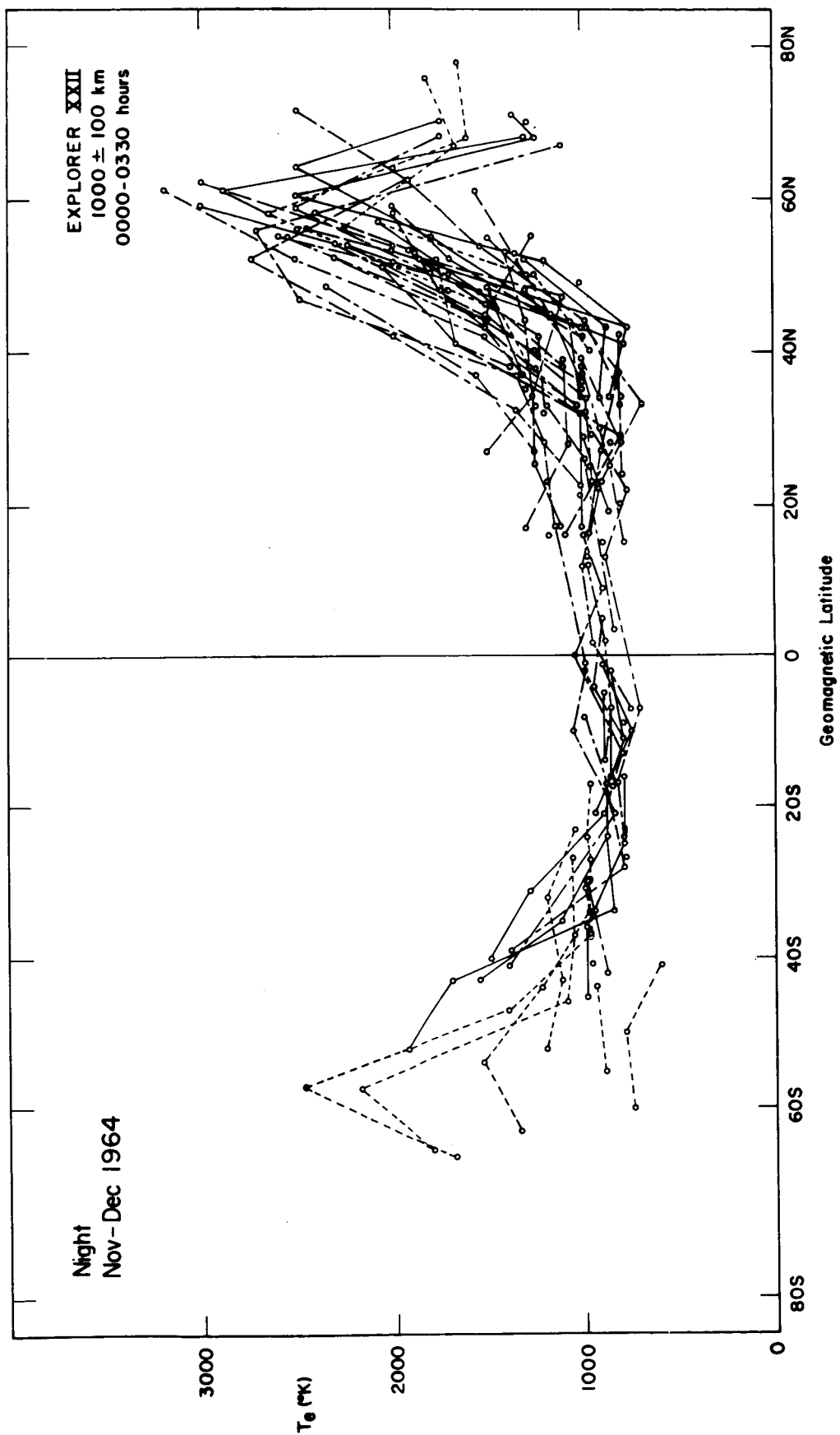
10

Figure 6—Raw values of T_e for same nighttime passes as employed for N_e data in figure 5
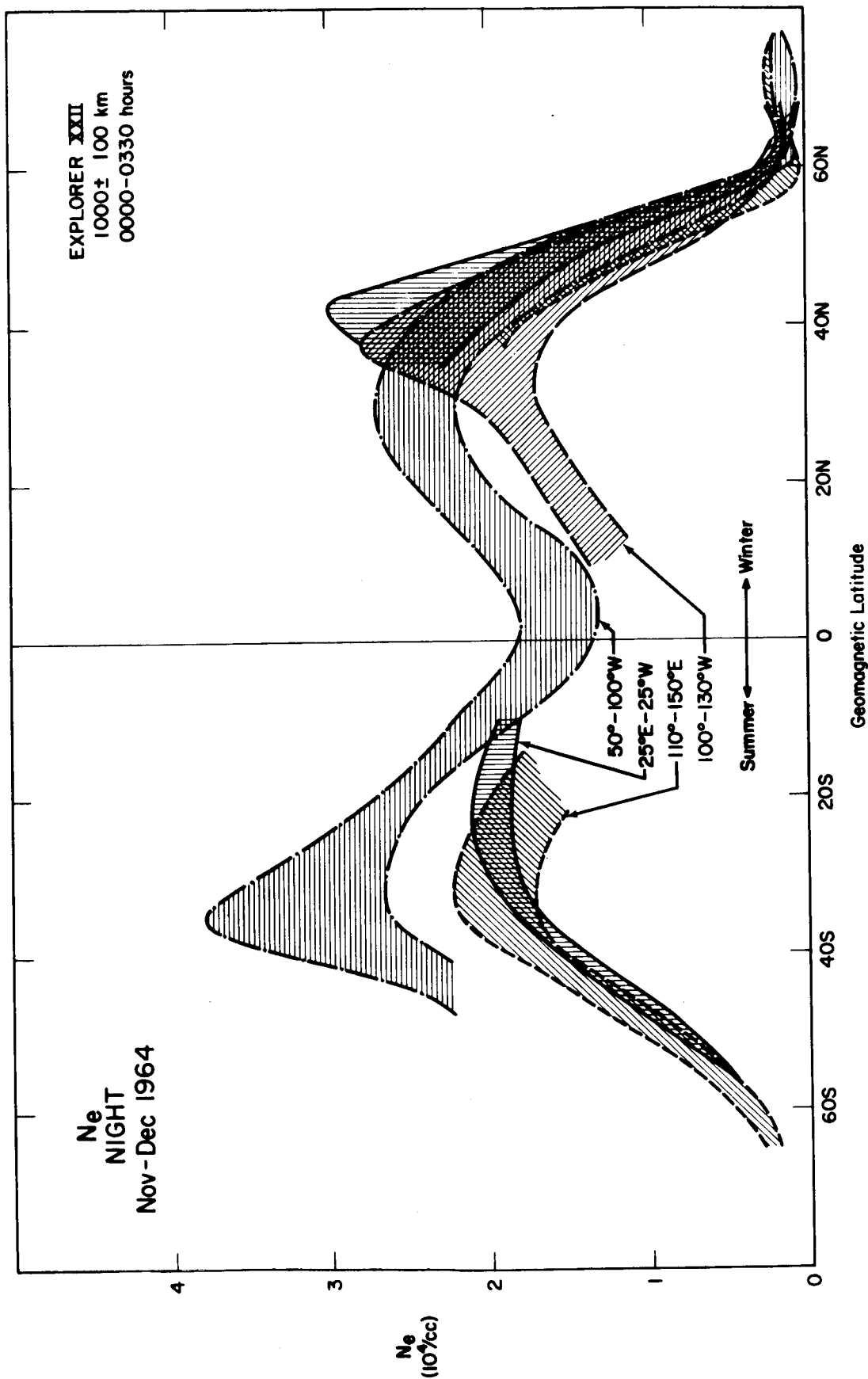
11

Figure 7—Gross latitudinal distribution of electrons in the nighttime ionosphere. The shaded areas represent the range of N_e in the given longitude ranges.
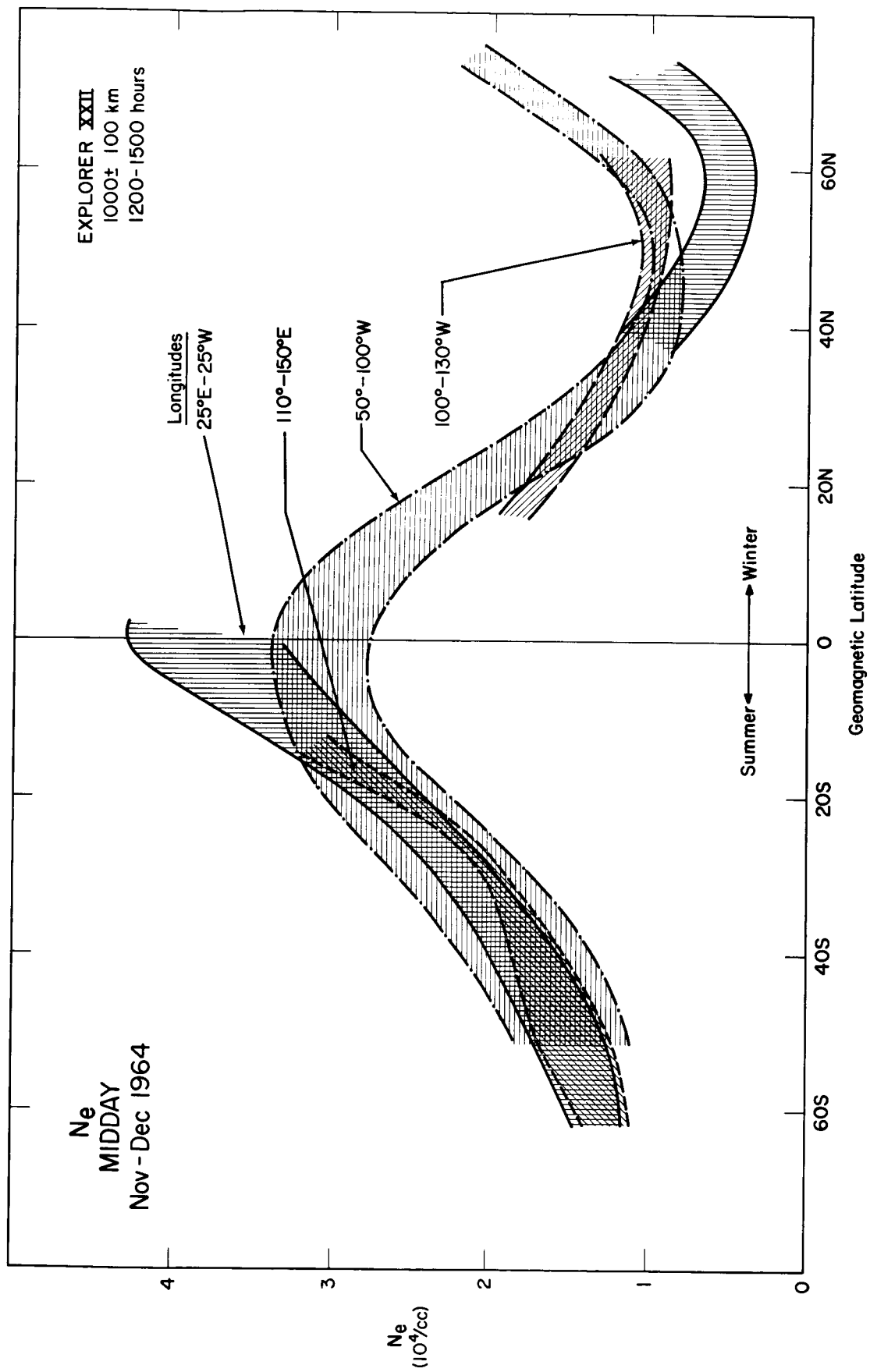
12

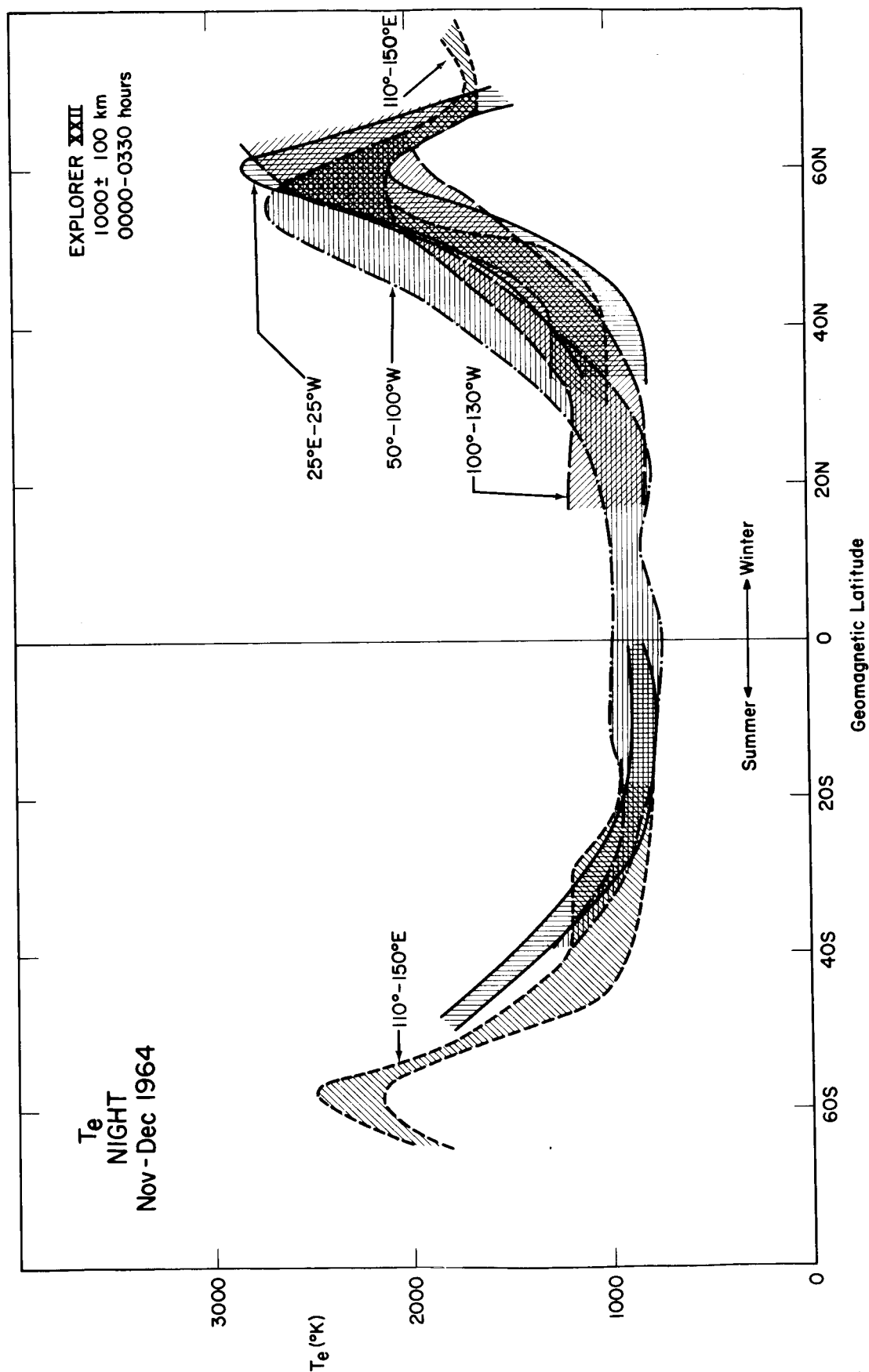Figure 9–Gross distribution of N_e in the daytime ionosphere

Figure 8—Gross distribution of T_e in the nighttime ionosphere
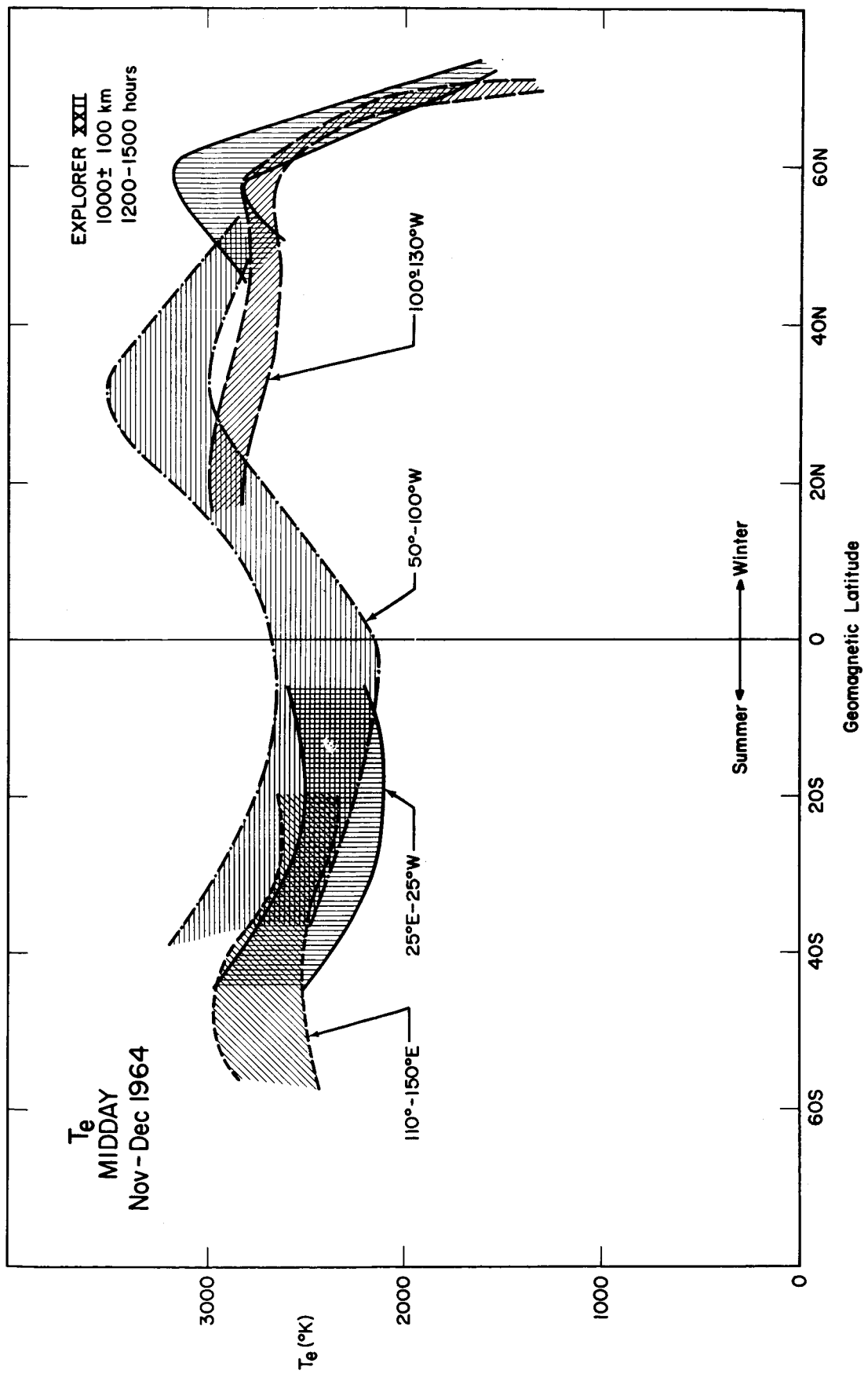
13

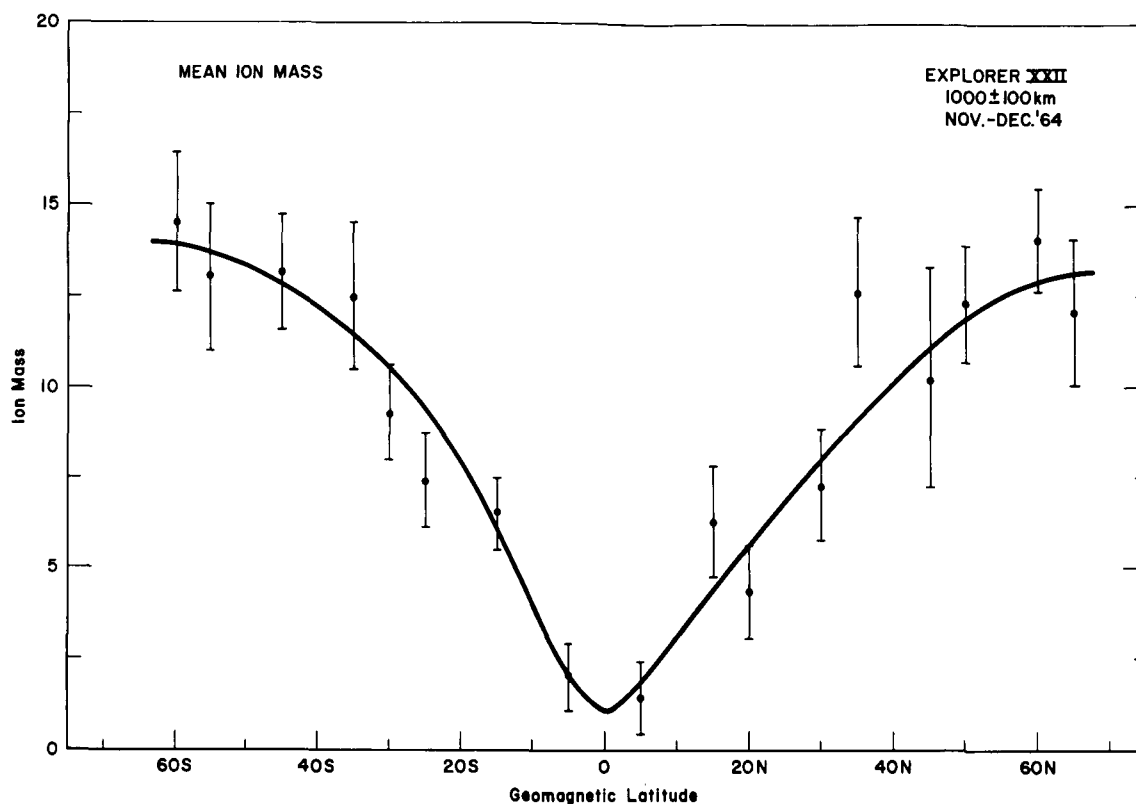Figure 10—Gross distribution of T_e in the daytime ionosphere

15

Figure 11—The mean ion mass (AMU) inferred from the slopes of the ion saturation regions of the daytime data

Local Time Behavior of T_e and N_e

Although data for a half rotation of the orbit plane (3 months) are not yet analyzed for all stations, it has been possible to analyze enough data to outline the diurnal behavior of the ionosphere at a few locations. Figure 12 shows the diurnal variation of T_e at mid latitudes near the 75th meridian. Most of the spread in the data arises from the wide longitude window employed to obtain sufficient point density. Figure 13 shows in addition the corresponding variation of N_e. Note that at mid latitudes, the nighttime electron concentration exceeds that found during the day. Figure 14 shows the corresponding diurnal variation of T_e near the 75th meridian in the northern and southern mid latitudes and at the equator.

Longitudinal Behavior

Although the ionosphere at the 1000 kilometer level appears to reflect primarily local time and latitudinal variations, longitudinal variability is also strong
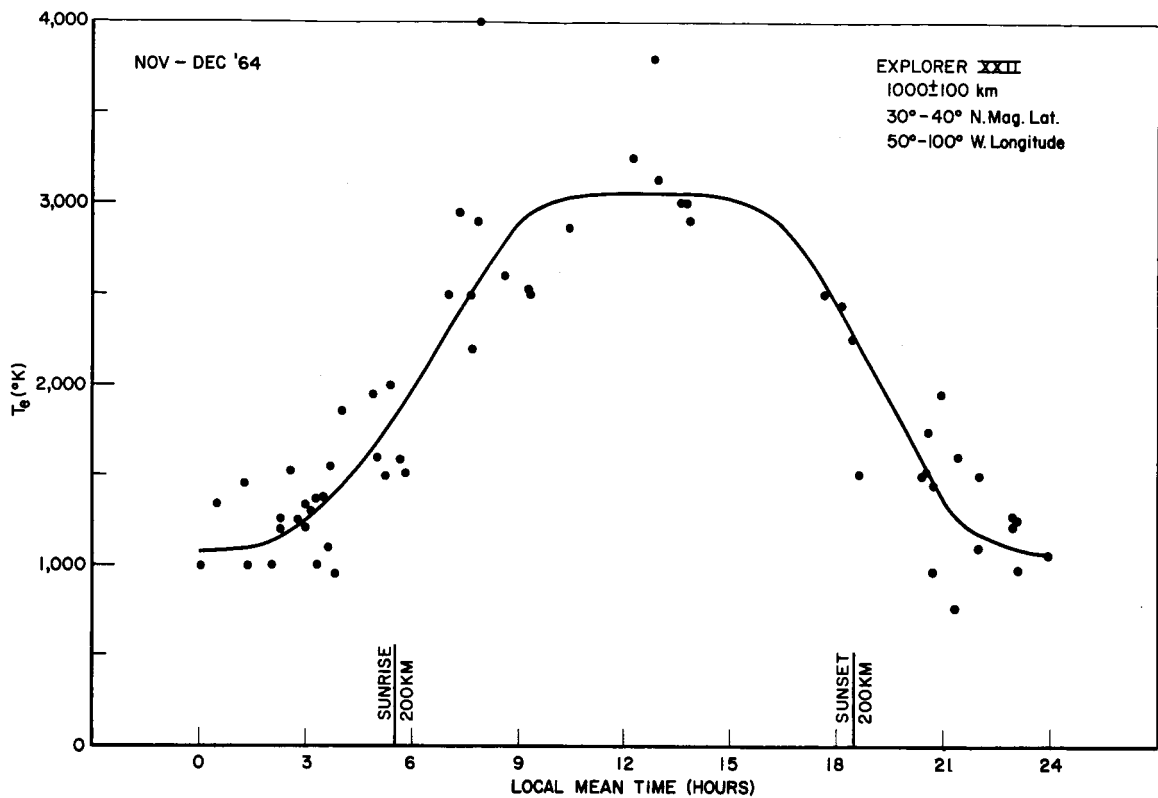
Figure 12—The diurnal variations of T_e at northern midlatitudes.

in some regions of the globe. The greatest effect is in the 25°E-25°W zone where both an equatorial enhancement and a high latitude deficiency are characteristic of the daytime ionosphere. Note that this is in the region just east of the Brazilian magnetic anomaly.

A second longitudinal irregularity occurs at night in the 50°-100°W zone where the southern hemisphere nocturnal maximum is enhanced by nearly a factor of two, and its northern counterpart is depressed and occurs at a somewhat lower latitude. Note that this region is at the western edge of the Brazilian anomaly. It seems probable that these longitudinal irregularities are related to the distortion of the earth's magnetic field in the region of the anomaly and its conjugate.

Small Scale Irregularities

On many occasions when the satellite was north of the auroral zone, the volt-ampere characteristics exhibited rapid fluctuations of the nature shown in
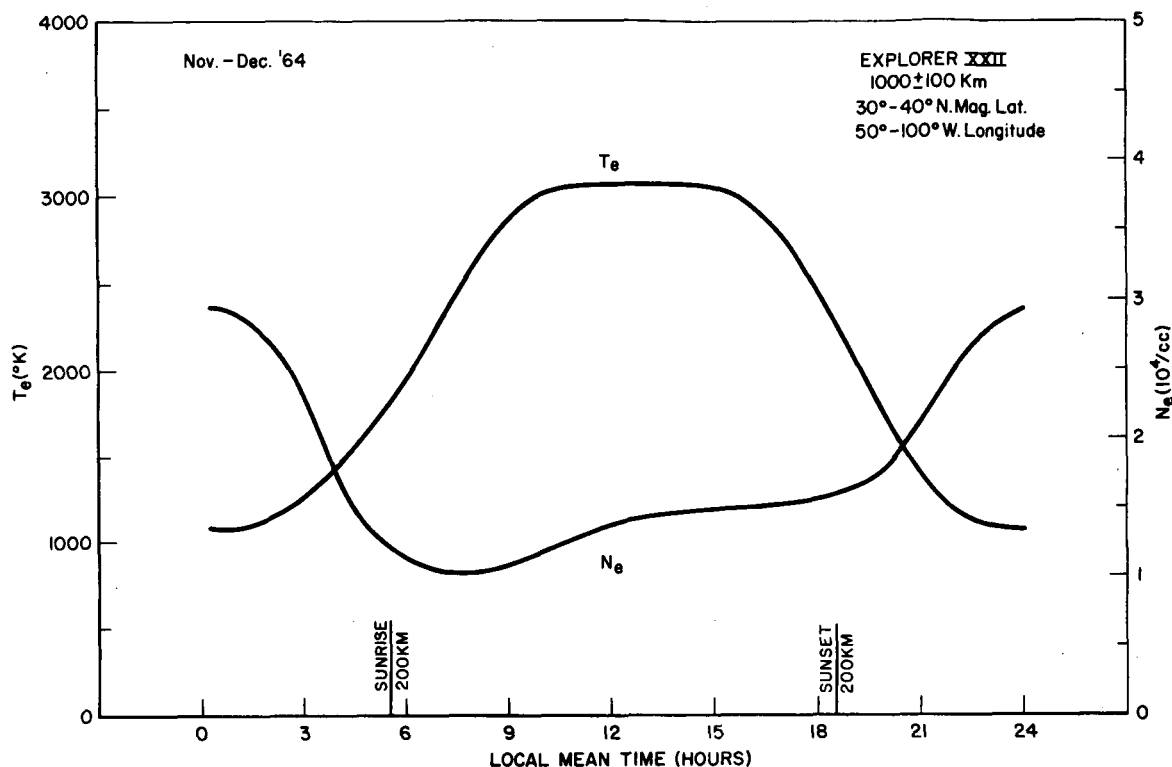
Figure 13—The diurnal variation of N_e and T_e at northern midlatitudes

Figure 15. When these small scale current variations occurred, they were visible on both detectors and probes. Since the normal operation of the measurement and telemetry systems is evident from the smoothness of the inflight current calibrations, these fluctuations can only be attributed to small scale variations in N_e along the orbit of the satellite. The horizontal dimensions of these irregularities are of the order of 300 meters and the magnitude may be as great as 30%. Figure 16 shows the locations of these occurrences. They are normally found on more than one burst when present at all. With a few exceptions, the irregularities occur above the auroral zone and present statistics suggest that they exist in about 10% of the passes, with a strong preference for the early morning hours (0000 - 0600). There appears to be little correlation with magnetic disturbances which were few during this period.

DISCUSSION OF RESULTS

The data reveal that the global structure of the ionosphere at 1000 km exhibits a high degree of variablity with respect to latitude, longitude and local time.
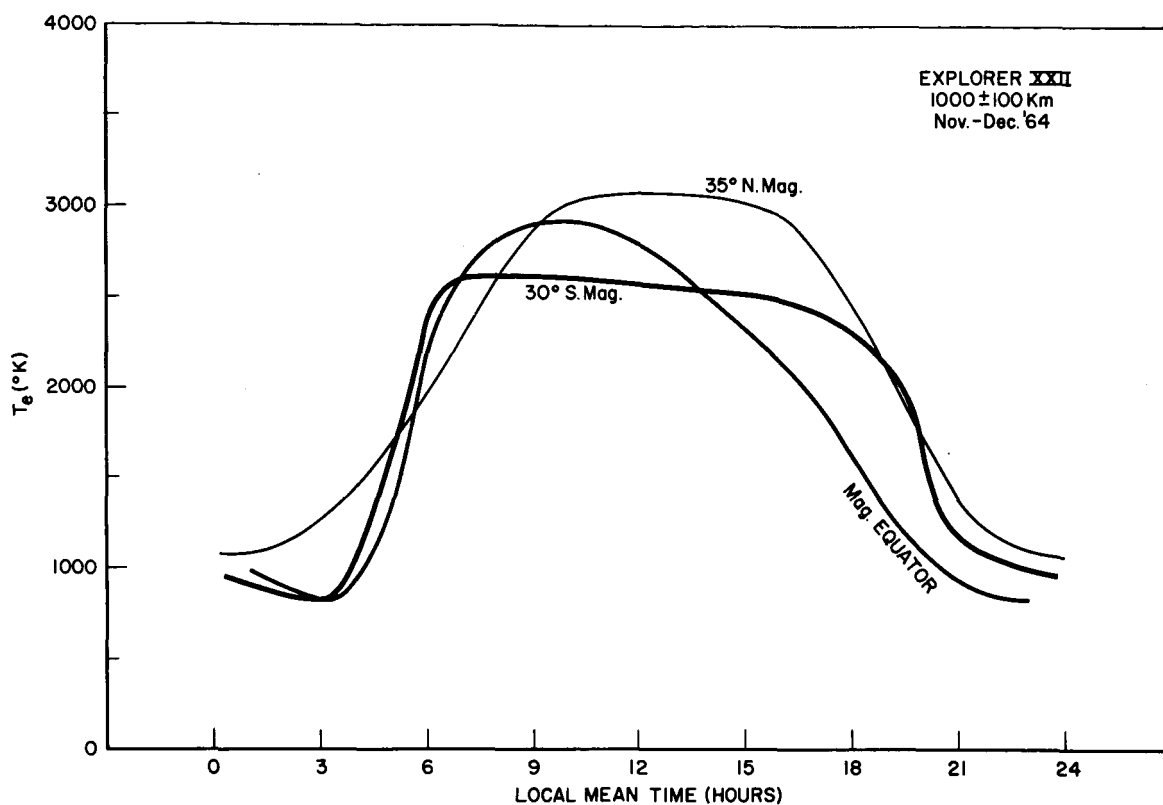
Figure 14-The dirunal variation of T_e at midlatitudes and at the equator at the 75th meridian.

The Electron Concentration

At midday (Figure 9), N_e exhibits a strong maximum at the magnetic equator, a result which is consistent with the Alouette topside sounder data (Lockwood and Nelms, 1964).[6] A general decrease in N_e with increasing latitude extends to a minimum at 60°N and S latitude where N_e is about one third its equatorial value.

At night (Figure 7), the equatorial maximum has given way to a pair of midlatitude maxima at 35°N and 35°S. The value of N_e at the equatorial trough is about one half of that at the maximum. This is not unlike the pattern shown by the Ariel satellite measurement of N_e for this altitude during northern summer of 1962 (Sayers, 1964).[7] This may therefore be a permanent feature of the nocturnal ionosphere.

These maxima observed at 35° latitude may be the nighttime counterpart of the equatorial anomaly present in the daytime at lower altitudes (see for example

Explorer XXII

BE-B

COL 573

300 meters

Hi Current Channel
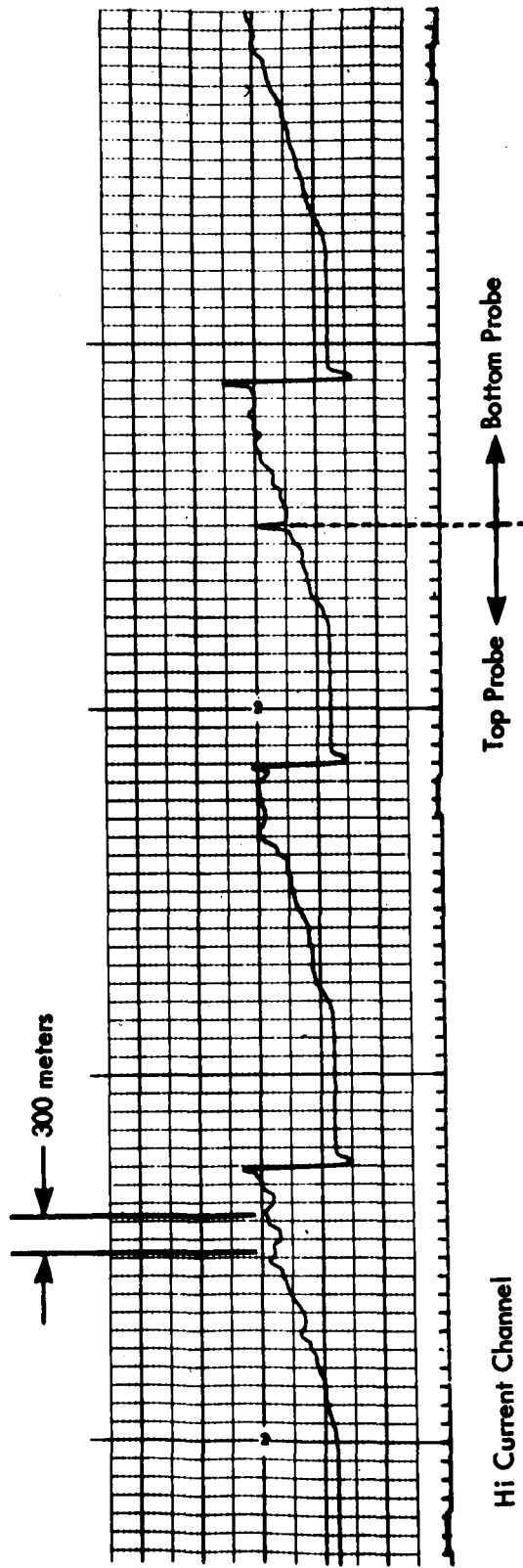
Top Probe ◄───► Bottom Probe

Figure 15–Volt-ampere characteristics exhibiting rapid fluctuations of N_e along the orbital path. Typical fluctuations are 100's of meters in dimension and have magnitudes of up to 30%.
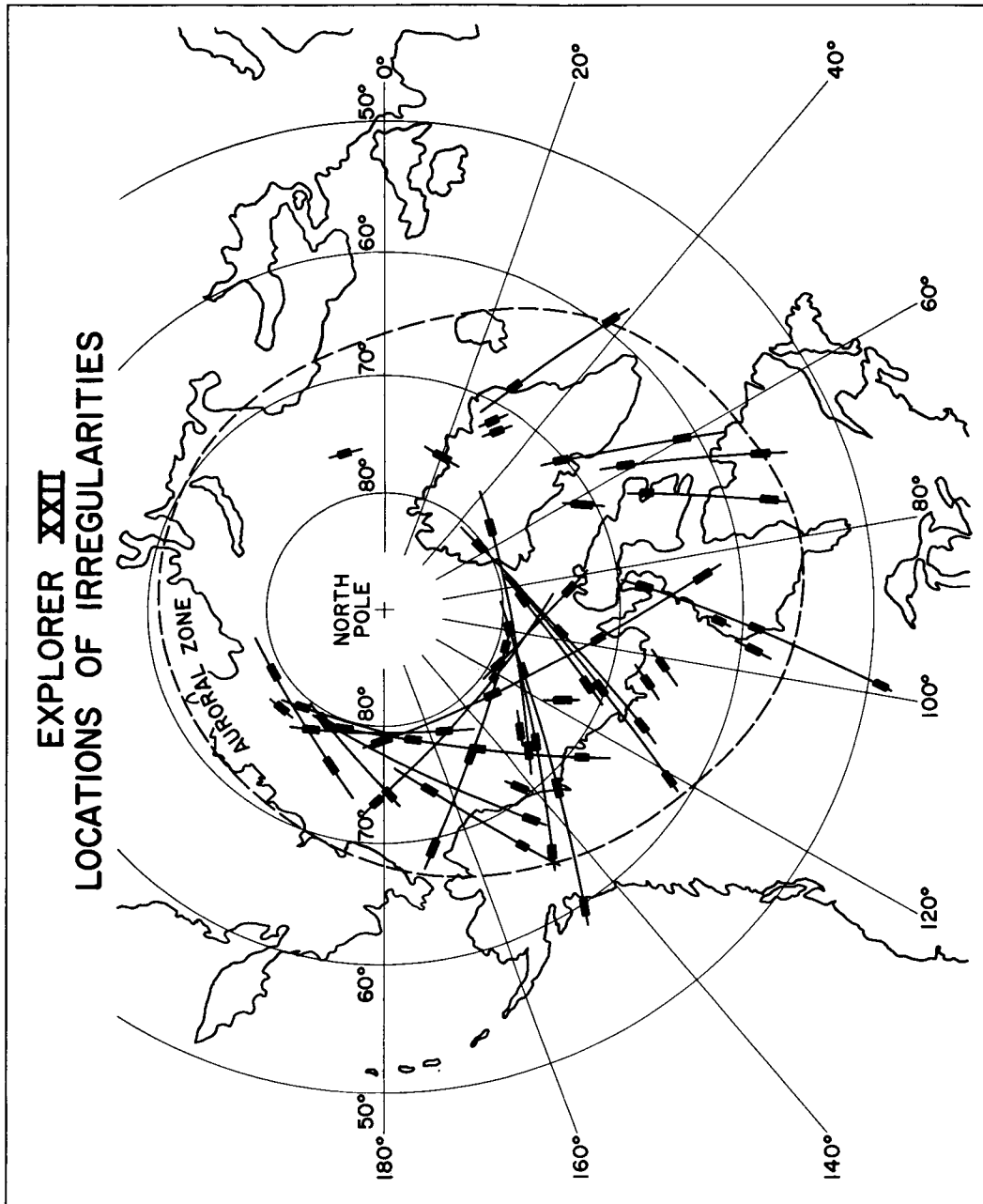
EXPLORER XXII
LOCATIONS OF IRREGULARITIES

Figure 16–Locations of small scale irregularities. Nearly all occur poleward of the auroral zone and in the early morning hours.

21

Goldberg and Schmerling, 1962).[8] King has pointed out (private communication) that the foF2 data from ground-based sounders show a general poleward movement of the maxima, which constitute the anomaly, through the afternoon and evening. Since the double maximum in the daytime anomaly has merged into a single maximum at the altitude of the Explorer XXII observations, we are unable to trace this poleward motion through the day. Instead, the maxima which we observe at 1000 kilometers seem to emerge in their equilibrium position near 35° latitude within a few hours after sunset.

Attempts to explain behavior of the daytime equatorial anomaly have been based on production and diffusion processes in the F-region. The identification of this anomaly as a major feature at night at higher altitudes suggests rather that the source of particles is in the protonosphere above the equator. Indeed, the daytime equatorial maximum at 1000 kilometers (Figure 9) assures a huge reservoir of electrons at higher altitudes in the protonosphere. At night this reservoir has nearly disappeared (Figure 7), and there seems little doubt that these electrons have diffused downward along the magnetic field lines to form the midlatitude maxima which are observed.

At higher latitudes an extraordinarily steep gradient reduces the concentration by nearly two orders of magnitude in less than 20° of latitude. The resulting minimum at 60° North, evident also in Aloutte data has been called the auroral trough (Muldrew, 1965: private communication). This also seems to be a permanent feature of the ionosphere, but is most discernible at night. The fact that the trough occurs at a magnetic latitude of 60° leads one to suspect that this is the same phenomena which produces the "knee whistlers" observed by Carpenter (1964)[9] near magnetic invariant L = 4. The polar cliff, an enhancement north of the auroral trough noted by Muldrew does not seem to be present at all longitudes (See Figure 5).

The high degree of symmetry about the magnetic equator which is evident in these N_e data makes it clear that the magnetic field of the earth exercises strong control over the global distribution of electrons, as has been evident to some degree from previous satellite data (Bowen et al. 1964),[10] (Sayers, 1964)[7] and (Brace et al. 1964),[3] though the global structure has not been displayed quite so clearly before. The approximate circularity of the orbit combined with its near polar nature, which is a highly advantageous feature of the Explorer XXII, enables a transparent latitudinal exposition of the ionospheric parameters measured without much reduction of the data.

It is interesting that the geomagnetic symmetry remains strong inspite of the extreme declination of the sun which was near the winter solstice during this period. Only a moderate seasonal asymmetry is evident at mid latitudes where N_e is about a factor of two larger in the summer hemisphere.

The Electron Temperature

A similar and undoubtedly closely related magnetic control is evident in the global distribution of electron temperature. At mid-day, T_e exhibits broad maxima at 40–50° latitude and a shallow minimum at the equator, variations which are generally inversely related to the variations in N_e. This is demonstrated best in Figure 17 which shows the daytime latitudinal behavior of the ionosphere averaged over all longitudes.

At night, the inverse relationship between electron temperature and concentration is limited to the higher latitudes as summarized in Figure 18. Because of the near vertical nature of the magnetic field lines at high latitudes, one expects the same general behavior at lower altitudes also. Explorer XVII data at College, Alaska indeed show elevated electron temperatures accompanied by depressed electron concentrations in the F_1 region (Brace et al. 1964),[3] and this is strong evidence for a nocturnal heat source there.

Heat Sources

Hanson (1963)[11] and Dalgarno et al. (1963)[12] have predicted that solar ultraviolet radiation produces photoelectrons which heat the ambient thermal
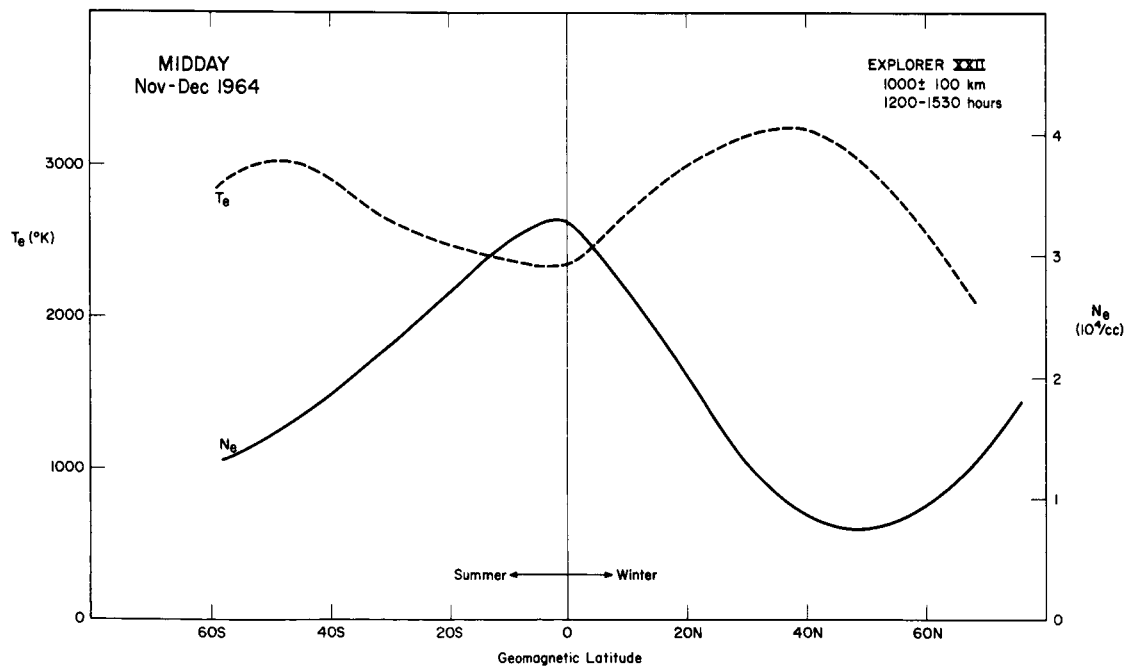

Figure 17–Midday values of T_e and N_e, averaged from data at all longitudes.
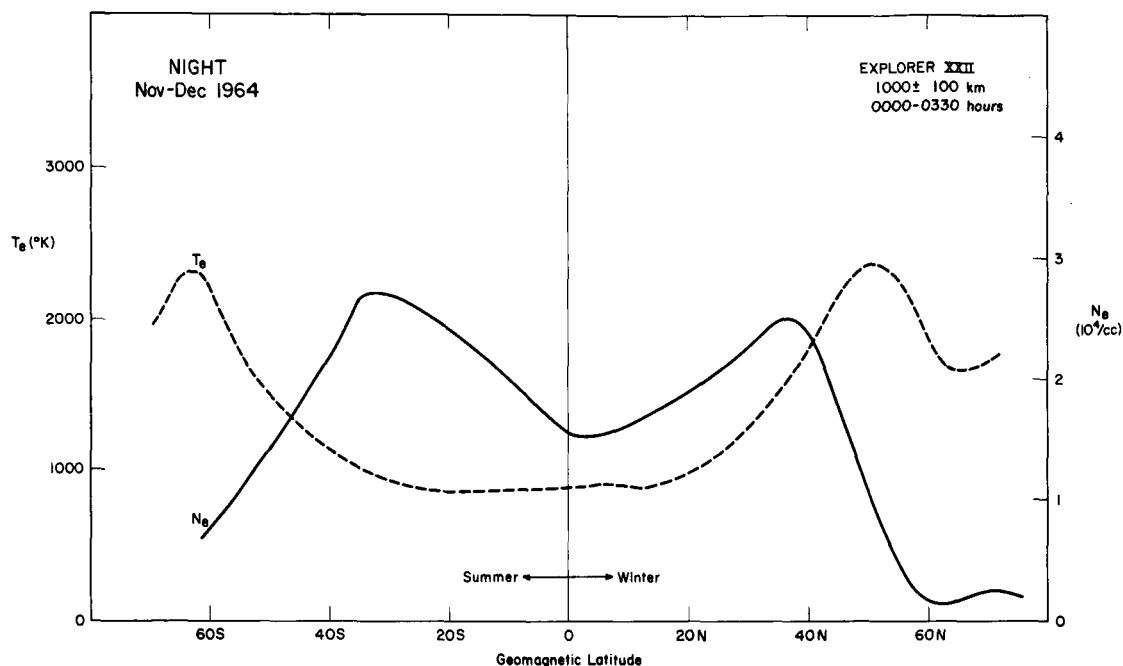
Figure 18—Nighttime values of T_e and N_e, averaged from data at all longitudes

electrons which in turn conduct their excess energy to neutral particles. In the F_1 region and below, the electrons are cooled primarily by their frequent collisions with neutral particles. Near the F_2 maximum, the neutral particle concentration is sufficiently low, so that electron cooling to the ions predominates. Geisler and Bowhill (1964)[13] have shown that, in the upper F region and exosphere, heat conduction to lower altitudes within the electron gas predominates the local heat loss.

When loss to neutrals predominates (F_1 region), the form of the local heating equation is

$$Q_e \, \alpha \, N_e N_n \, (T_e - T_n)$$

where N_n and T_n are the neutral particle concentration and temperature respectively, and when loss to ions predominates (F_2 region)

$$Q_e \, \alpha \, N_e^2 (T_e - T_i) / T_e^{3/2},$$

REFERENCES

1. Aviation Week and Space Technology, pp. 30, September 21 (1961).

2. Missiles and Rockets, pp. 11 October 19, (1964).

3. Brace, L. H., N. W. Spencer, and A. Dalgarno, Planet, Space Sci. (to be published, 1965).

4. Spencer, N. W., L. H. Brace, G. R. Carignan, D. R. Taeusch and H. Niemann. J. Geophys. Res., June (1965).

5. Mott-Smith, H. M. and I. Langmuir, Phys. Rev, 28, 727 (1926).

6. Lockwood, G. E. K. and G. L. Nelms, Journal of Atmos. and Terr. Physics, 26, 569, (1964).

7. Sayers, J. Proc. Roy. Soc. A, 281, 450 (1964).

8. Goldberg, R. A. and E. R. Schmerling, J. Geophys. Res. 68, 1927, (1963).

9. Carpenter, D. L., J. Geophys. Res., 68, 1675, (1963).

10. Bowen, P. J., R. L. F. Boyd, C. L. Henderson and A. P. Willmore, Proc. Roy. Soc. A, 281, 526 (1964).

11. Hanson, W. B., Space Research III (North Holland-Amsterdam) Edited by W. Priester, (1963).

12. Dalgarno,A.,M. B. McElroy and R. J. Moffett, Planet Space Sci. 11, 463, (1963).

13. Geisler, J. E. and S. A. Bowhill, Aeronomy Report No. 5, University of Illinois, Urbana, Illinois, January (1965).

and when conductivity controls the cooling rate (upper F region and exosphere) Q_e is independent of N_e. Thus one expects T_e and N_e to vary approximately inversely in the F_1 region and inversely as the square in the F_2 region. In the upper F-region, however, there is little local heating. Therefore T_e is controlled by heat conductivity to the lower F-region, and N_e is controlled by diffusion and charge transport processes, and the relation between T_e and N_e is not controlled by energy input locally.

Future Analysis

Further analysis of the data from the sunset and sunrise periods, which have not been stressed here, is expected to expand our understanding of the dynamic response of the upper ionosphere to the elevation of the sun. Data from later orbital plane precession cycles, which has not yet been analyzed or is not yet obtained, will permit us to repeat the profiles given in this paper so as to reveal the seasonal control which may be evident in the global pattern.